Ordu Üniversitesi Bilim ve Teknoloji Dergisi
Ordu Üniv. Bil. Tek. Derg.

Ordu University Journal of Science and Technology
Ordu Univ. J. Sci. Tech.

E-ISSN: 2146-6459 2023, 13(2), 174-192 Araştırma Makalesi / Research Article
https://doi.org/10.54370/ordubtd.1308195

Computational Insights in Drug-likeness and ADMT Properties of -dienes Resemble of Geranial

Goncagül Serdaroğlu[1]

[1]Sivas Cumhuriyet University, Mathematics and Science Education, Sivas

Geliş Tarihi / Received Date: 31.05.2023 Kabul Tarihi / Accepted Date: 13.06.2023

Abstract

This research aims to analyze the drug development potential of geranial, a naturally occurring compound known for its medicinal properties, through in-depth ADMT (Absorption, Distribution, Metabolism, and Toxicity) profiling and Density Functional Theory (DFT) calculations, at B3LYP/6-311G** level and basis set. The optimized and confirmed structures of the data set were used for further computations. The FMO "Frontier Molecular Orbital" energies and MEP "Molecular Electrostatic Potential" were considered to elucidate the possible reactivity features and regions of the molecules, respectively. Concurrently, DFT calculations helped to elucidate the compound's electronic properties and structural stability, further affirming its suitability for drug development. These findings emphasize the potential of compounds structurally related to geranial in the pharmaceutical field and underline the necessity of similar evaluations for novel drug candidates, ensuring safety and efficacy while mitigating potential risks to human health and the environment.

Keywords: geranial, ADMT study, DFT computations

Geranial benzeri -dienlerin İlaç Benzerliği ve ADMT Özelliklerine İlişkin Hesaplamalı Analizler

Öz

Bu araştırma, tıbbi özellikleriyle bilinen, doğal olarak oluşan bir bileşik olan geranialin (sardunya) ilaç geliştirme potansiyelini, derinlemesine ADMT (Absorbsiyon, Dağıtım, Metabolizma ve Toksisite) profili oluşturma ve B3LYP/6-311G** fonksiyon ve temel setinde, Yoğunluk Fonksiyonel Teorisi (DFT) hesaplamaları yoluyla analiz etmeyi amaçlamaktadır. Veri setinin optimize edilmiş ve onaylanmış yapıları daha sonraki hesaplamalar için kullanıldı. FMO "Frontier Molecular Orbital" enerjileri ve MEP "Moleküler Elektrostatik Potansiyel" sırasıyla moleküllerin olası reaktivite özelliklerini ve bölgelerini aydınlatacak şekilde değerlendirildi. Ayrıca, DFT hesaplamaları bileşiğin elektronik özelliklerinin ve yapısal stabilitesinin aydınlatılmasına yardımcı oldu ve ilaç geliştirmeye uygunluğunu doğruladı. Bu bulgular, farmasötik alanda geranial ile yapısal olarak ilişkili bileşiklerin potansiyelini vurgulamakta ve insan sağlığına ve çevreye yönelik potansiyel riskleri azaltırken güvenlik ve etkinliği sağlayan yeni ilaç adayları için benzer değerlendirmelerin gerekliliğinin altını çizmektedir.

Anahtar Kelimeler: geranial, ADMT çalışması, DFT hesaplamaları

Sorumlu Yazar / Corresponding Author: Goncagül Serdaroğlu goncagul.serdaroglu@gmail.com

Introduction

Geranial, also known as citral, is a naturally occurring organic compound found in various essential oils, including lemongrass, lemon, and orange (Gaonkar et al., 2016; Wohlmuth et al., 2006). Geranial-based molecules, derivatives, and analogs have garnered significant attention due to their unique chemical properties and diverse applications, particularly in the field of medicine. Furthermore, it is a volatile aldehyde with a distinct citrus aroma and is widely used in the fragrance and flavor industries (Burdock et al., 2009) as well as food additives (Ruiz et al., 2008; Sharmeen et al., 2021). Its characteristic citrus scent provides a fresh and invigorating experience, contributing to its widespread use in various consumer products. Additionally, geranial possesses antimicrobial (Viktorová et al., 2020), antifungal (Ju et al., 2020), and insecticidal (Oyedeji et al., 2020; Plata-Rueda et al., 2020) properties, making it an effective natural preservative and repellent.

In recent years, the medicinal importance of geranial and its derivatives has been extensively studied and researchers have discovered a range of potential therapeutic applications for these molecules (Bailly 2020, Li et al., 2015; Zeng et al., 2023). In this respect, Studies have shown that geranial exhibits significant anticancer activity by inducing apoptosis (programmed cell death) in cancer cells, inhibiting tumor growth, and suppressing metastasis (Balusamy et al., 2020; Samarghandian et al., 2014; Silva et al., 2021). Its cytotoxic effects on cancer cells have made it a promising candidate for the development of novel chemotherapeutic agents. Moreover, geranial-based molecules have demonstrated potent anti-inflammatory and analgesic properties, which have been found to inhibit the production of inflammatory mediators and reduce pain in various experimental models (Adorjan et al., 2010; Bouyahya et al., 2022; Ortiz et al., 2010). These findings suggest that geranial and its derivatives hold promise for the development of new anti-inflammatory drugs and pain management strategies. Furthermore, geranial has shown antimicrobial activity against a wide spectrum of bacteria, fungi, and parasites. It exhibits inhibitory effects against several pathogenic organisms, including Staphylococcus aureus, Candida albicans, and Plasmodium falciparum, the parasite responsible for malaria (Oladeji et al., 2020; Sharma et al., 2023; Tchoumbougnang et al., 2005). The antimicrobial potential of geranial-based molecules has led to their investigation as alternative agents for the treatment of infectious diseases, particularly those caused by drug-resistant microorganisms.

In light of the diverse properties and medicinal importance of geranial-based molecules, this paper aims to provide an overview of their main characteristics and therapeutic potential. For this aim, we performed the DFT computations based on the B3LYP hybrid function using the 6-311G** basis set to determine and evaluation of the electronic structure underlying the reactivity tendency. Also, the ADMT features of the compounds have been used to evaluate pharmacokinetics, drug-likeness, and toxicity possibility in addition to the water solubility and lipophilicity to discuss the challenges and prospects for developing geranial-based molecules as pharmaceutical agents. By gaining a deeper understanding of the main properties and medicinal significance of geranial and its derivatives, we hope to pave the way for further research and development in this promising field. The potential applications of geranial-based molecules in various therapeutic areas make them an intriguing subject for exploration and hold the potential to make a significant impact on human health.

Computational Methods

DFT Study

The G09W (Frisch et al., 2013) and GaussView 6.0.16 (Dennington et al., 2016) packages were used for all DFT computations at the B3LYP (Becke 1993; Lee et al., 1988) /6-311G** (Raghavachari et al., 1980; McLean et al., 1980) level of theory maintaining default (Kudin et al., 2002; Li et al., 2006) settings and for demonstrating the optimized structures and FMO plots, respectively.

As known well, the thermodynamic quantities have been assessed depending on the principles of quantum statistics (Hill 1962; McQuarrie 1973). In this way, the Q "partition function" is crucial in

determining thermodynamic properties through specific equations defined below. In such asymmetric top systems, the vibrational degree of freedom equals 3N-6, because the molecular system allows for movement (three degrees) and rotation (three degrees) along three distinct axes. Thus, it is crucial to be aware that the differences in the quantities of thermodynamic properties for all asymmetric top molecules stem from the vibrational movements, as the contributions from translational and rotational movements are akin due to specific physical constants. The vibrational partition function is formulated as below, and its contribution to thermodynamic properties is essential in assessing chemical properties (Herzberg 1964; Hill 1962; McQuarrie 1973; Serdaroglu & Durmaz 2010).

$$Q = Q_{trans.}\, x\, Q_{rot.}\, x\, Q_{vib.}\, Q_{elec.}$$

$$Q_{vib.} = \prod_{j=1}^{3N-6} \frac{e^{-\Theta_{v,j}/2T}}{\left(1-e^{-\frac{\Theta v,j}{T}}\right)}$$

Here, Evib. "vibrational thermal energy", Svib. "vibrational entropy", and Cvvib. "vibrational heat capacity" are calculated by the following equations (Herzberg 1964; Hill 1962; McQuarrie 1973).

$$E_{vib.} = Nk \sum_{j=1}^{3N-6} \left(\frac{\Theta_{v,j}}{2} + \frac{\Theta_{vj}\, e^{-\Theta_{v,j}/T}}{\left(1 - e^{-\frac{\Theta v,j}{T}}\right)} \right)$$

$$S_{vib} = Nk \sum_{j=1}^{3N-6} \left[\frac{\Theta_{v,j}/T}{\left(e^{\Theta_{v,j}/T} - 1\right)} - ln\left(1 - e^{-\Theta_{v,j}/T}\right) \right]$$

$$Cv_{vib.} = Nk \sum_{j=1}^{3N-6} \left[\left(\frac{\Theta_{vj}}{T}\right)^2 \frac{e^{\Theta_{vj}/T}}{\left(e^{\Theta_{v,j}/T} - 1\right)^2} \right]$$

The terms disclose as $\Theta_{vj} = \frac{h\nu_j}{k}$ "the vibrational temperature", h→ "Planck constant", k→ "Boltzmann constant", and ν_j→" j^{th} fundamental frequency".

Koopmans` theorem defined the I "ionization energy" and A "electron affinity" (Koopmans 1934) depending on the energies of the frontier molecular orbital. From the I and A values, the global reactivity values can be calculated by the following equations.

I= -E_{HOMO}

A= -E_{LUMO}

$$\chi = -(\frac{I+A}{2})$$

$$\eta = \frac{I-A}{2}$$

$$\omega = \frac{\mu^2}{2\eta}$$

$$\Delta N_{max} = \frac{I + A}{2(I - A)}$$

$$\omega^+ \approx (I + 3A)^2/(16(I - A))$$

$$\omega^- \approx (3I + A)^2/(16(I - A))$$

$$\Delta\varepsilon_{back-donation} = -\frac{\eta}{4}$$

Here, the symbols show that χ → "electronic chemical potential" η → "global hardness", ω → "electrophilicity", ΔN_{max} → "the maximum charge transfer capability index" (Janak 1978; Parr et al., 1983; Parr et al., 1999; Pearson 1986; Perdew et al., 1982; Perdew et al., 1983), ω- "the electrodonating power" and ω+ "the electroaccepting power" (Gazquez et al., 2007), and $\Delta E_{back\text{-}donat.}$ "back-donation energy" (Gomez et al., 2006).

Lipophilicity and Water Solubility Features

The lipophilicity indices were ascertained utilizing five methodologies, which were ILOGP (Daina et al., 2014), XLOGP3 (Cheng et al., 2007), WLOGP (Wildman et al., 1999), MLOGP (Lipinski et al., 2001), and SILICOS-IT (Silicos-it) utilized through the execution of SwissADME (Daina et al., 2017). It is well acknowledged that the lipophilicity parameter (Log P), founded on the concentration of a distinct neutral molecular system in octanol (Co) and water (Cw), is defined as follows.

$$Log\ P_{o/w} = Log\ \frac{C_o}{C_w}$$

The water solubility (Log S) was also calculated by using different approaches defined by Delaney (Delaney et al., 2004) and Ali et al. (Ali et al., 2012). Accordingly, the approach ESOL "Estimated SOLubility" defined by Delaney (Delaney et al., 2004) is given depending on the molecular features, which are "Molecular weight, MWT", "Rotatable bonds, RB", "Aromatic proportion, AP" as follows

$$\text{Log } Sw = 0.16\text{-}0.63 \text{ clogP - } 0.0062 \text{ MWT} + 0.066 \text{ RB - } 0.74 \text{ AP (ESOL)}$$

On the other hand, the benchmark study performed by Ali et al. (Ali et al., 2012) revealed that water solubility depends on the phenolic parameters remarkable which are the number of the aromatic -OH group(s), in addition to the melting point and TPSA, as follows.

$$\text{logS} = -1.0239 \text{ logP} - 0.0148 \text{ TPSA} - 0.0058 \text{ (m.p. (C)} - 25) + 0.3295 \text{ aroOHdel} + 0.5337 \text{ (ALI)}$$

Absorption, Distribution, Metabolism, Druglikeness, and Toxicity Study

The drug-likeness features of the data set were considered on the basis of Lipinski (Lipinski et al., 2001), Ghose (Ghose et al., 1999), Veber (Veber et al., 2002), Egan (Egan et al., 2000), and Muegge (Muegge et al., 2001) rules. Also, the Abbott score (Martin, 2005) for bioavailability investigations of data set scores was used via SwissADME (Daina et., 2017) tools. The adsorption, distribution characteristics, metabolism, and possible toxicity features of the data set were determined by ADMETLab 2.0 (ADMETlab 2.0).

Result and Discussion

Molecule Geometry and Thermochemical Properties

The thermochemical and physical properties are critical as these aspects govern the fundamental physical and chemical characteristics of matter, influencing phenomena from routine chemical reactions to advanced processes in the pharmaceutical design, material science, and environmental chemistry (Serdaroğlu 2017; Serdaroğlu 2011a; Serdaroğlu 2011b). The calculated quantities of the studied compounds (Fig. 1) were presented in Table 1.

The dipole moment and polarizability of the compounds D1-D5 were determined as D2(4.837)> D1(3.060)> D5(1.477)> D3(1.389)> D4(0.330) and D5(134.850)> D4(130.332)> D1(122.071)> D2(118.499)> D3(108.089), respectively. Here, the -C≡N group substitution on the -diene bone made an increase in the dipole moment due to the lone pair electrons of nitrogen. Furthermore, the ΔE, ΔH, and ΔG quantities of the compounds were predicted as the following orders of D5 (-580.336463)< D1 (-541.050353)< D4 (-522.256208)< D2 (-444.708110)< D3(-427.673040), D5 (-

580.319444)< D1 (-541.035022)< D4 (-522.239504)< D2 (-444.693855)< D3 (-427.659033), and D5 (-580.382097)< D1 (-541.093717)< D4 (-522.301559)< D2 (-444.749447)< D3 (-427.713702), respectively. The $\Delta E_{ther.}$ (kcal/mol) was calculated as D4 (182.305)> D5 (178.519)> D1 (160.225)> D3 (152.395)> D2 (149.172), which the main contribution to each of them stemming from the vibrational freedom degrees. Subsequently, the $Cv_{vib.}$ (cal/molK) of the compounds were found to be D5 (50.591)> D4 (49.311)> D1 (45.387)> D2 (41.368)> D3 (40.303). The S and S_{vib} (cal/molK) were predicted as D5 (131.864)> D4 (130.606)> D1 (123.534)> D2 (117.002)> D3 (115.060) and D5(58.182)> D4 (57.347)> D1 (50.678)> D2 (45.080)> D3 (43.896), respectively. Accordingly, these observations, facilitated by precise calculations and predictions, reveal the influence of molecular modifications such as the -C≡N or -OCH3 substitution on the -diene bone. Subsequently, the results would be hoped to ultimately aid in predicting and manipulating the compounds' behaviors for specific applications such as smart material design and therapeutic purposes.

Table 1. The Calculated Physiochemical Values at B3LYP/6-311G** Level

	D1	D2	D3	D4	D5
DM (debye)	3.060	4.837	1.389	0.330	1.477
α (au)	122.071	118.499	108.089	130.332	134.850
ΔE (au)	-541.050353	-444.708110	-427.673040	-522.256208	-580.336463
ΔH (au)	-541.035022	-444.693855	-427.659033	-522.239504	-580.319444
ΔG (au)	-541.093717	-444.749447	-427.713702	-522.301559	-580.382097
$\Delta E_{thermal}$ (kcal/mol)	160.225	149.172	152.395	182.305	178.519
$\Delta E_{vib.}$ (kcal/mol)	158.447	147.395	150.618	180.527	176.742
Cv (cal/molK)	51.348	47.330	46.265	55.273	56.553
$Cv_{vib.}$ (cal/molK)	45.387	41.368	40.303	49.311	50.591
S (cal/molK)	123.534	117.002	115.060	130.606	131.864
S_{vib} (cal/molK)	50.678	45.080	43.896	57.347	58.182

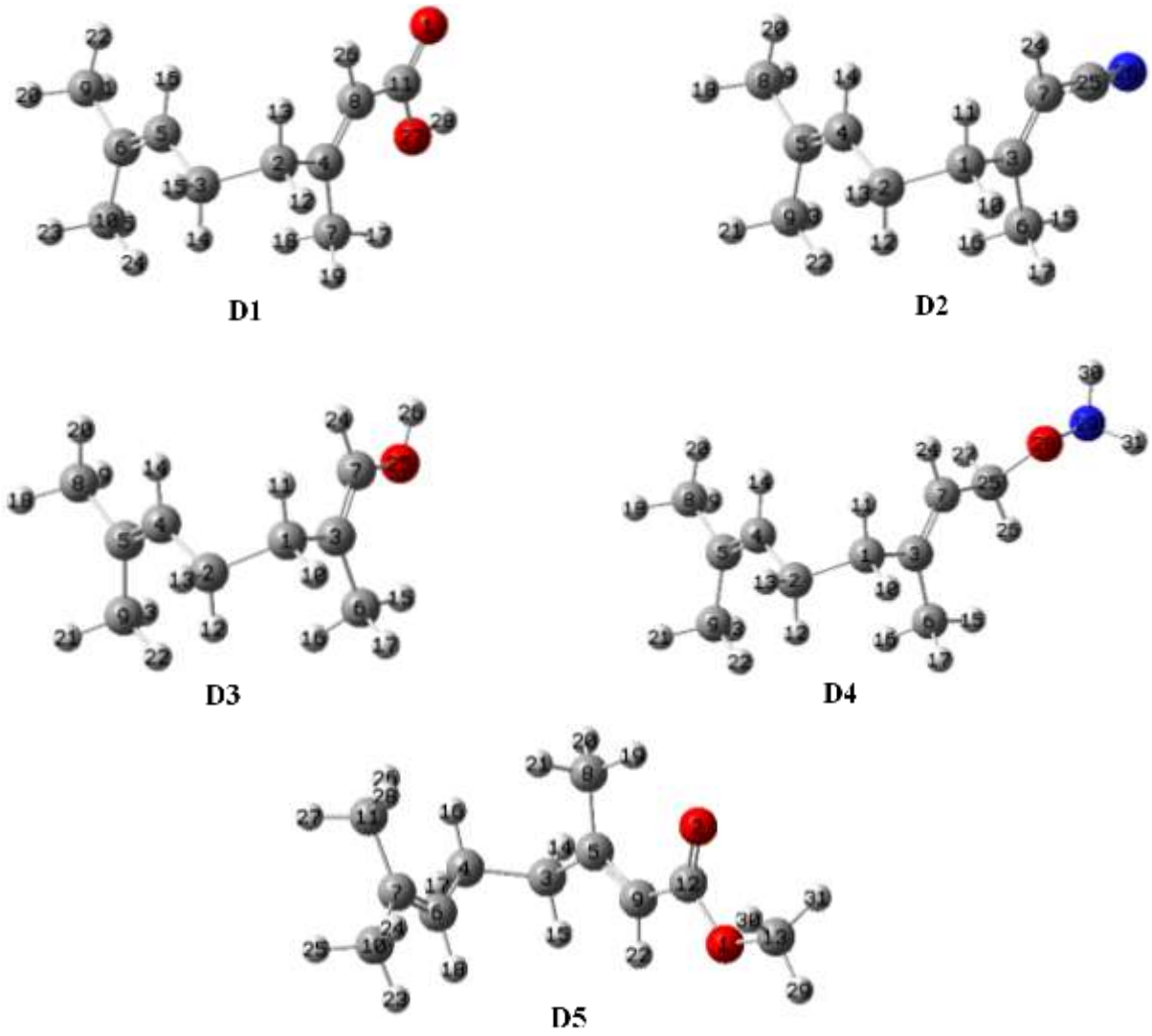

Figure 1. The Optimized Structures of the Studied-dienes

Lipophilicity and Water Solubility Features

In the realm of drug discovery and development, two key factors are fat-solubility (lipophilicity) and the water-solubility of organic compounds. Lipophilicity greatly affects a drug's absorption, distribution, metabolism, and excretion (Lin et al., 1997), with highly lipophilic drugs possessing the potential for toxicity due to their accumulation in the body's fatty tissues (Jackson et al., 2017). On the other hand, water solubility plays a significant role in drug formulation, delivery, and bioavailability, with challenges arising for drugs with either too high or too low water solubility. Both lipophilicity and water-solubility have a bearing on drug-drug interactions and chemical stability, impacting drug efficacy, safety, and overall applicability (Carpenter et al., 1997).

From Table 2, the Log Po/w (iLOGP) indices were calculated as D5 (3.05)> D4 (2.81)> D2 (2.63)> D3 (2.55)> D1 (2.13), whereas lipophilicity depended on the XLOGP3 approach was determined as D5 (3.42)> D4 (3.35)> D2 (3.29)> D3 (3.21)> D1 (3.09). On the other hand, the WLOGP and MLOGP approaches revealed that the following changes in the lipophilicity predicted in D2 (3.20)> D3 (3.19)> D5 (2.85)> D1 (2.76)> D4 (2.57) and D5 (2.67)> D2 (2.49)> D4 (2.47)> D1 (2.38)> D3 (2.28), respectively. The Log Po/w showed some different order depending on the approach used to predict the indices. The order of average Log Po/w of the compounds was determined as D5 (2.91)> D2 (2.82)> D3 (2.63)> D1 (2.58)> D3 (2.47). The varying Log Po/w values determined by different

methods (iLOGP, XLOGP3, WLOGP, MLOGP) underscore the critical role of lipophilicity in the behavior and potential interactions of compounds D1-D5.

For all approaches, the compounds D1-D5 were found to be soluble in the water. Namely, the solubility (mg/mL)x10^{-1} values of the compounds D1-D5 depend on the ESOL were determined as follows D1 (4.57)> D3 (4.10)> D4 (3.62)> D2 (3.42)> D5 (2.92), whereas solubility (mg/mL)x10^{-2} was calculated as D3 (6.91)> D2 (5.12)> D1 (4.84)> D5 (4.06)> D4 (2.89) based on the Ali approach. On the other hand, the solubility score obtained from SILICOS-IT was changed in the order of D1 (6.73)> D3 (5.22)> D4 (2.62)> D5 (1.42)> D2 (1.19). Despite the varying indices calculated by different predictive methods, it is clear that all compounds would be soluble in the water.

Table 2. Physicochemical Properties, Lipophilicity, and Water Solubility Characteristics

	D1	D2	D3	D4	D5
Physicochemical properties	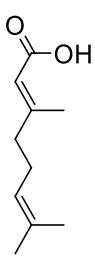	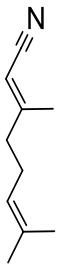		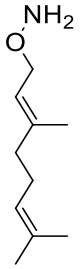	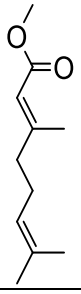
Name	(E)-3,7-dimethyloct a-2,6-dienoic acid	(E)-3,7-dimethyloct a-2,6-dienenitrile	(E)-2,6-dimethylhepta-1,5-dien-1-ol	O-(3,7-dimethylocta-2,6-dien-1-yl)0020hydroxyl amine	methyl (E)-3,7-dimethyloct a-2,6-dienoate
Formula	C10H16O2	C10H15N	C9H16O	C10H19NO	C11H18O2
Molecular weight (g/mol)	168.23	149.23	140.22	169.26	182.26
Num. heavy atoms	12	11	10	12	13
Num. arom. heavy atoms	0	0	0	0	0
Fraction Csp3	0.50	0.50	0.56	0.60	0.55
Num. rotatable bonds	4	3	3	5	5
Num. H-bond acceptors	2	1	1	2	2
Num. H-bond donors	1	0	1	1	0
Molar Refractivity	51.01	48.98	46.00	53.03	55.33
TPSA (Å²)	37.30	23.79	20.23	35.25	26.30
Lipophilicity					
Log $P_{o/w}$ (iLOGP)	2.13	2.63	2.55	2.81	3.05
Log $P_{o/w}$ (XLOGP3)	3.09	3.29	3.21	3.35	3.42
Log $P_{o/w}$ (WLOGP)	2.76	3.20	3.19	2.57	2.85
Log $P_{o/w}$ (MLOGP)	2.38	2.49	2.28	2.47	2.67
Log $P_{o/w}$ (SILICOS-IT)	1.96	2.47	1.91	1.72	2.54
Consensus Log $P_{o/w}$	2.47	2.82	2.63	2.58	2.91
Water Solubility					
Log S (ESOL)	-2.57	-2.64	-2.53	-2.67	-2.79
Solubility (mg/mL)x10^{-1}	4.57	3.42	4.10	3.62	2.92
Class	Soluble	Soluble	Soluble	Soluble	Soluble
Log S (Ali)	-3.54	-3.46	-3.31	-3.77	-3.65
Solubility (mg/mL)x10^{-2}	4.84	5.12	6.91	2.89	4.06
Class	Soluble	Soluble	Soluble	Soluble	Soluble
Log S (SILICOS-IT)	-1.40	-2.10	-1.43	-1.81	-2.11
Solubility (mg/mL)	6.73	1.19	5.22	2.62	1.42
Class	Soluble	Soluble	Soluble	Soluble	Soluble

**TPSA "topological polar surface Area" was calculated based on polar fragments that contributed to the polar surface.*

Absorption, Distribution, Metabolism, Druglikeness, and Bioavailability Study

In the domain of pharmaceutical research, parameters such as absorption, distribution, metabolism, bioavailability, and drug-likeness are fundamental. From this perspective, we determined these key parameters to evaluate their significance in the landscape of drug discovery and design and presented Table 3.

From Table 3, all compounds were found to be promising structures in view of Caco-2 Pe, MDCK Pe., Pgp-inh., Pgp-subs., and HIA. Namely, the Caco-2 Pe. indices of the compounds were determined higher than the optimal value (-5.15) in the following order of D3 (-5.071)< D1 (-4.789)< D4 (-4.475)< D2 (-4.32)< D5 (-4.299). Also, MDCK Pe. ($x10^{-5}$) cm/s indices implied that all compounds would show high passive permeability by the order of D4 (3.4)> D2=D3 (2.5)> D5 (2.3)> D1 (1.3). The Pgp-inh. and Pgp-subs. indexes of the compounds were determined in the ranks of 0.000-0.016 and 0.005-0.101, respectively. In addition, the HIA values of the compounds D1-D5 were estimated in the range of 0.003-0.009. For all compounds, the $F_{30\%}$ scores give the green alarm predicted in the range of 0.006-0.074. The $F_{20\%}$ values of the compounds D1, D2, D4, and D5 were estimated in the range of 0.023-0.135, while it for D3 was found to be 0.738 by a red alarm.

Except for D4 (81.33%), the other compounds presented high PPB % scores which were greater than 90% and which implied that there could be a lower therapeutic feature. For all compounds, VD scores were calculated in the region of the optimal limits (0.04-20L/kg). However, the BBB Pen. values of D1 and D5 were estimated at 0.194 and 0.157, while this indice for D2-D4 were determined at 0.962, 0.724, and 0.974, respectively. Also, Fig. 2 supported the BBB Pen. the capability of all compounds because they would be placed in the yolk region of the BOILED-EGG. The fractional unbonded form in the plasma for D2 would be at a low level (4.750%), while D4 (22.81) could be said that a high level in plasma as unbonded. The other compounds as unbonded would be in the plasma at a medium level (5~20%). In addition, the metabolism scores of the compounds implied that all compounds might have been suitable structures for both substrate and inhibitor against the different lines of the P450s. The calculated ADM scores, as these crucially influence a compound's therapeutic efficacy and its interaction with metabolic enzymes like P450s, thereby playing a pivotal role in the design and/or modification of potential drugs.

Table 3. Absorption, Distribution, and Metabolism Scores

	D1	D2	D3	D4	D5
Absorption					
Caco-2 Pe.	-4.789	-4.32	-5.071	-4.475	-4.299
MDCK Pe. ($x10^{-5}$) cm/s	1.3	2.5	2.5	3.4	2.3
Pgp-inh.	0.001	0.002	0.0	0.016	0.003
Pgp-subs.	0.022	0.005	0.011	0.101	0.011
HIA	0.006	0.003	0.005	0.009	0.005
$F_{20\%}$	0.135	0.023	0.738	0.034	0.08
$F_{30\%}$	0.051	0.007	0.026	0.006	0.074
Distribution					
PPB %	95.10	96.67	94.00	81.33	97.52
VD (L/kg)	0.554	2.892	4.807	1.437	2.696
BBB Pen.	0.194	0.962	0.724	0.974	0.157
Fu %	13.47	4.750	11.95	22.81	10.12
Metabolism					
CYP1A2 inh.	0.088	0.974	0.214	0.760	0.922
CYP1A2 subs.	0.190	0.849	0.574	0.424	0.655
CYP2C19 inh.	0.028	0.952	0.028	0.237	0.593
CYP2C19 subs.	0.078	0.831	0.831	0.539	0.869
CYP2C9 inh.	0.123	0.559	0.019	0.072	0.466
CYP2C9 subs.	0.832	0.948	0.956	0.789	0.889
CYP2D6 inh.	0.342	0.150	0.053	0.054	0.055
CYP2D6 subs.	0.180	0.453	0.683	0.476	0.246
CYP3A4 inh.	0.016	0.139	0.009	0.034	0.065
CYP3A4 subs.	0.097	0.280	0.122	0.216	0.243

** Permeability, Pe; Penetration, Pen, Inhibitor, Inh; Substrate, subs. MDCK, Madin-Darby canine kidney; HIA, Human Intestinal Absorption; PPB, Plasma Protein Binding; VD, Volume Distribution; BBB, Blood-Brain Barrier Penetration; Fu, fraction unbound in plasma; hERG, human ether-a-go-go related gene; H-HT, Human Hepatotoxicity; DILI, Drug-Induced Liver Injury; FDAMDD, FDA Maximum (Recommended) Daily Dose.*

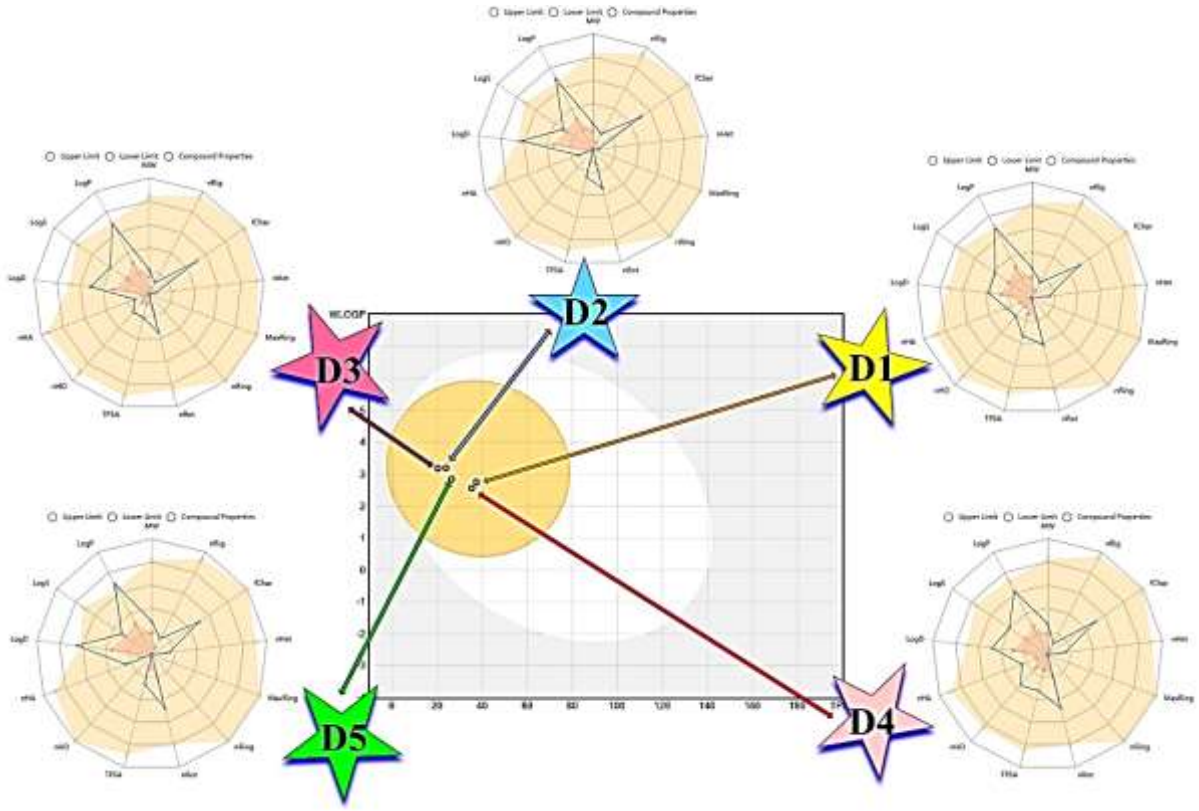

Figure 2. BOILED-Egg Model and Pharmacokinetic Radar Graphs

Toxicity Study

One of the goals of drug discovery and development is to find therapeutic agents that are safe, effective, and improve patient outcomes. In this regard, it also involves a rigorous toxicity assessment of potential drug candidates and an evaluation of their 'drug-likeness'. The computational tools are used to anticipate toxicity scores, including medical and environmental risks, and identify favorable pharmacokinetic and pharmacodynamic properties. Here, the calculated toxicity results were presented in Table 4.

In terms of the hERG Blockers, DILI, AMES, Rat Oral Acute, and FDAMDD, there would be a low (or no) toxic effect possibility for all compounds. On the other hand, the H-HT scores revealed that all compounds could be toxic due to the higher toxicity index values predicted in the range of 0.839-0.898. Except for the D3 (0.317) at a medium level, the other compounds would have also presented an adverse effect in terms of eye Irritation. The D1 (0.892), D2 (0.910), and D4 (0.849) would have been a higher toxic possibility for eye corrosion, whereas D3 (0.017) and D5 (0.700) could be caused to low and medium level toxic effect, respectively. The D1 (0.817), D4 (0.926), and D5 (0.921) could be adversely in terms of skin sensitivity, whereas this possibility for the compounds D2 (0.520) and D3 (0.433) was determined at a medium level. The carcinogenicity indices revealed that D4 (0.107) and D5 (0.237) could have a low severe effect, while D1 (0.327) and D2 (0.422) could have medium-level toxicity. The D2 (0.920) would-be toxic at a high level in terms of the respiratory, D5 could be moderate level toxic, and the others probably could have a low toxic effect.

In view of the environment, the BCF scores of all compounds were determined lower than the threshold value (log BCF< 3.3) (McGeer et al., 2003; Nendza et al., 2010). The IGC50, LC50FM, and LC50DM values were determined in the ranks of 2.327-3.429, 3.469-5.735, and 4.465-6.040, respectively. In the view of the Tox21 pathway, the D1 would be toxic at a moderate level for NR-ER (0.350) and a high level toxic for SR-HSE (0.719), fortunately, there would be no toxic effect for the

others. The D2 could display a harmful effect in terms of the NR-ER-LBD (0.479) only. The D3 (0.628) and D4 (0.531) would be harmful to SR-HSE at a medium size. On the other hand, the D5 would be adverse at a high level to SR-HSE (0.739) and might be toxic for NR-ER-LBD (0.352) at medium size. From the results gathered in this study, we hope this work will underline the importance of toxicity assessment in future research and development efforts, facilitating the creation of safer, more efficacious therapeutic agents and contributing to the mitigation of potential risks to both human health and the environment.

Table 4. Toxicity Values

	D1	D2	D3	D4	D5
Medicinal					
hERG Blockers	0.007	0.020	0.066	0.016	0.014
H-HT	0.868	0.895	0.839	0.898	0.873
DILI	0.244	0.056	0.031	0.027	0.059
AMES Tox.	0.006	0.049	0.003	0.044	0.008
Rat Oral Acute Tox.	0.028	0.038	0.018	0.019	0.017
FDAMDD	0.027	0.053	0.208	0.226	0.049
Skin Sens.	0.817	0.520	0.433	0.926	0.921
Carcinogencity	0.327	0.422	0.752	0.107	0.237
Eye Corrosion	0.892	0.910	0.017	0.849	0.700
Eye Irritation	0.988	0.989	0.317	0.981	0.959
Respiratory Tox.	0.218	0.920	0.145	0.147	0.303
Environmental					
BCF	0.390	0.998	0.191	2.677	0.828
IGC_{50}	2.811	2.743	2.327	3.429	2.871
$LC_{50}FM$	3.554	4.073	3.469	5.735	4.195
$LC_{50}DM$	4.465	5.395	5.331	6.040	5.671
Tox21 Pathway					
NR-AR	0.010	0.014	0.009	0.004	0.008
NR-AR-LBD	0.004	0.005	0.003	0.003	0.005
NR-AhR	0.009	0.005	0.019	0.025	0.006
NR-Aromatase	0.006	0.011	0.004	0.009	0.011
NR-ER	0.350	0.077	0.095	0.061	0.078
NR-ER-LBD	0.143	0.479	0.010	0.010	0.352
NR-PPAR-gamma	0.005	0.011	0.003	0.003	0.006
SR-ARE	0.243	0.069	0.028	0.225	0.181
SR-ATAD5	0.005	0.006	0.005	0.006	0.009
SR-HSE	0.719	0.189	0.628	0.531	0.739
SR-MMP	0.024	0.013	0.016	0.033	0.010
SR-p53	0.011	0.050	0.007	0.034	0.020

**The abbreviations are defined as: Tox, Toxicity; sens, Sensitization; BCF, the unit of bioconcentration factors, IGC50, LC50FM, and LC50DM is given in -Log10[(mg/L)/(1000xMW)].*

FMO (Frontier Molecular Orbital) Analysis and MEP (Molecular Electrostatic Potential)

For a long time, the FMO analysis and MEP graphs are powerful theoretical tools used in the field of computational chemistry to study the electronic structure and reactivity of molecules (Erdoğan 2021; Hsissou et al., 2021; Serin 2023; Serin 2022; Serin et al., 2022;), providing insights into their chemical properties and interactions.

From Table 5, the order of the H (-I) and L (-A) (eV) of the compounds was calculated as D3 (-5.715)> D4 (-6.381)> D5 (-6.524)> D1 (-6.583)> D2 (-6.731) and D3 (0.634)> D4 (0.338)> D5 (-1.087)> D1 (-1.213)= D2 (-1.213), respectively. Accordingly, the global reactivity indices obtained from these values were changed in the following orders.

ΔE (L-H) (eV): D4 (6.719)> D3 (6.349)> D2 (5.518)> D5(5.438)> D1 (5.370)

μ (eV): D3 (-2.540)> D4 (-3.022)> D5 (-3.806)> D1 (-3.898)> D2 (-3.972)

η (eV): D4 (3.359)> D3 (3.174)> D2 (2.759)> D5 (2.719)> D2 (2.685)

ω (eV): D2 (0.105)> D1 (0.104)> D5 (0.098)> D4 (0.050)> D3 (0.037)

ω+ (au): D1 (0.045)= D2 (0.045)> D5 (0.040)> D4 (0.010)> D3 (0.005)

ω- (au): D2 (0.191)> D1 (0.188)> D5 (0.180)> D4 (0.121)> D3 (0.099)

$\Delta N_{max.}$ (eV): D1 (1.452)> D2 (1.440)> D5 (1.400)> D4 (0.899)> D3 (0.800)

$\Delta E_{back.}$ (eV): D1 (-0.671)> D5 (-0.680)> D2 (-0.690)> D3 (-0.794)> D4 (-0.840)

From obtained results, the D4 would tend to interact with the external molecular system more than the intramolecular interactions due to its highest ΔE value, and vice versa for D1. Considering the μ (eV) values, D2 could be more stable and D3 would be less stable structure. Furthermore, D4 was predicted the hardest molecule and D2 was found to softer one among the compounds. Concerning the electrophilicity feature, D2 could be said to present a more electrophilic character and D3 would have a less electrophilic character. The electrodonating power of all compounds would predominate on the electroaccepting potency. Moreover, D1 would have a higher charge transfer capability among the compounds and also it would gain more stability by way of the back donation. From Fig. 3, D1 and D5 would present similar HOMO densities, which were towards the dimethyl terminals of each molecule, whereas their LUMO would expand towards terminals -COO. For D2, the HOMO would be expanded over the surface except for the methyl group that was neighbor to the -CN group whereas the LUMO density would be distributed towards the half part where the -CN group substituted. The HOMO for D3 could be localized over the half part of the molecule toward the -OH terminal, whereas the LUMO would separate partially towards the -OH terminal and mainly localized on the remaining part. For D4, the HOMO would also have expanded toward -ONH2, whereas the LUMO would also distribute mainly over -ONH2 and slightly on the remaining part of the compound. Also, the surround of the O atom of the -C=O group for both D1 and D5 was covered by red color (V<0), which was a marker of the electron-rich region as a function of the electrostatic potential on the total density surface. The blue color for both D1 and D3 molecules would be appeared on the H atom of the -OH group, as expected. Moreover, the red color for D2 would be placed around the N atom of the -CN group. For the D4 molecule, the red color appeared on the central region of the compound whereas the moderate blue color covered the Hs of the -NH2 group.

Table 5. The Quantum Chemical Reactivity Values

	D1	D2	D3	D4	D5
H (-I) (eV)	-6.583	-6.731	-5.715	-6.381	-6.524
L (-A) (eV)	-1.213	-1.213	0.634	0.338	-1.087
ΔE (L-H) (eV)	5.370	5.518	6.349	6.719	5.438
μ (eV)	-3.898	-3.972	-2.540	-3.022	-3.806
η (eV)	2.685	2.759	3.174	3.359	2.719
ω (eV)	0.104	0.105	0.037	0.050	0.098
ω^+ (au)	0.045	0.045	0.005	0.010	0.040
ω^- (au)	0.188	0.191	0.099	0.121	0.180
$\Delta N_{max.}$ (eV)	1.452	1.440	0.800	0.899	1.400
$\Delta E_{back.}$ (eV)	-0.671	-0.690	-0.794	-0.840	-0.680

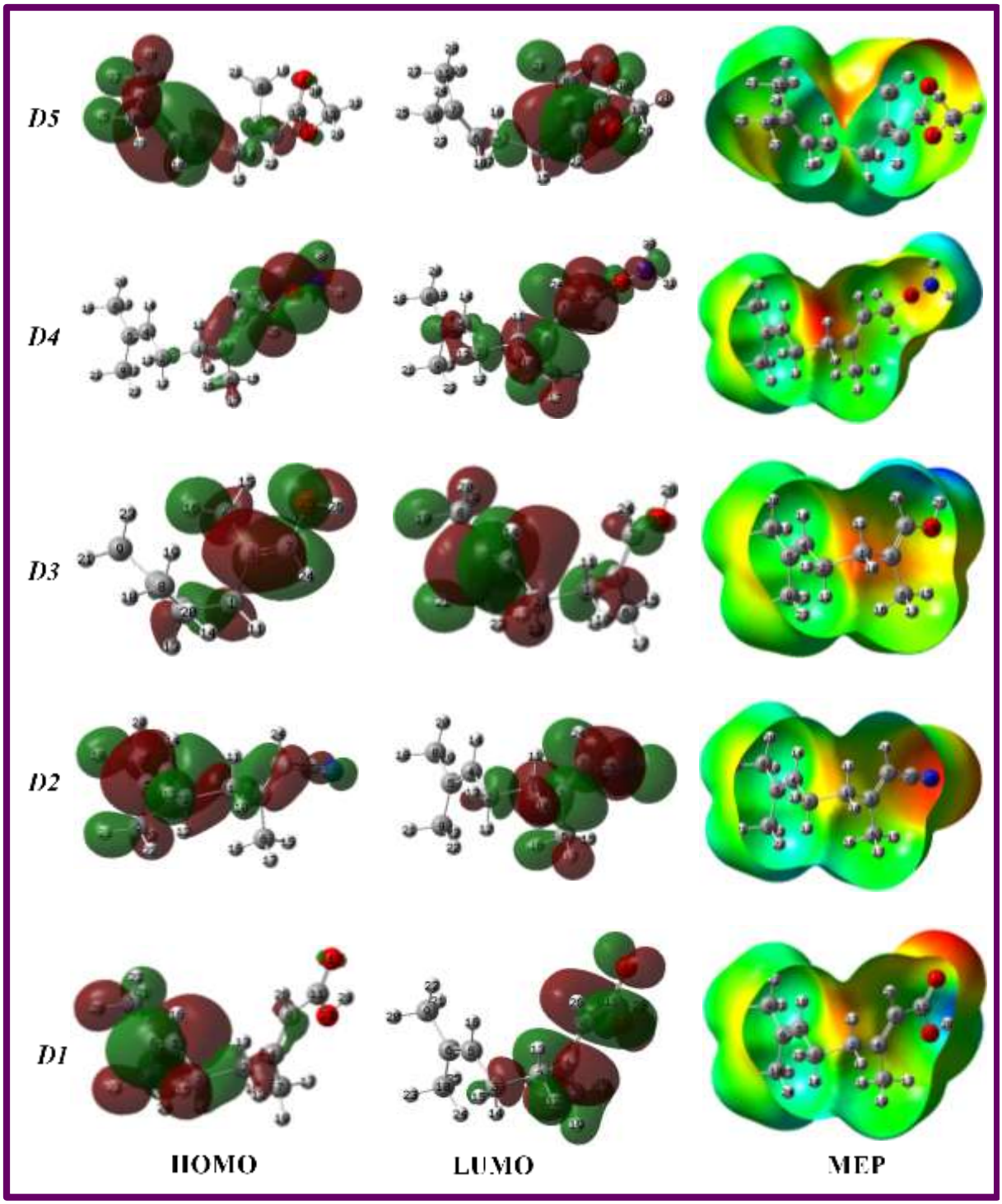

Figure 3. HOMO& LUMO (isoval:0.02), and MEP (isoval:0.0004) Plots

Conclusions

In this study, extensive computational investigations were conducted to assess the ADMT (absorption, distribution, metabolism, and toxicity) properties of the -diene derivatives. After optimizing and confirming the structures, various properties such as lipophilicity, water solubility, drug-likeness, and bioavailability were evaluated. Additionally, the potential toxicity from medicinal and environmental perspectives was considered. Structural factors influencing these properties were determined through FMO and MEP analyses as well as the global reactivity parameters. From FMO analyses, D4 was determined to have the highest ΔE value and thereby it would prefer to interact

with the external molecular systems more than the others. Furthermore, D1 would have a higher charge transfer capability among the compounds and also it would gain more stability by way of the back donation. The compounds exhibited promising structures concerning Caco-2 Pe, MDCK Pe, Pgp-inh, Pgp-subs, and HIA. All compounds showed low or no toxicity in hERG Blockers, DILI, AMES, Rat Oral Acute, and FDAMDD assessments. However, they exhibited potential toxicity based on the H-HT scores, with higher toxicity index values ranging from 0.839 to 0.898. Eye irritation was expected for all compounds except D3, while D1, D2, and D4 had a higher likelihood of causing eye corrosion. D1, D4, and D5 showed adverse effects on skin sensitivity. Carcinogenicity indices indicated varying levels of toxicity. Some compounds had high respiratory toxicity, while others had low or moderate toxic effects. In terms of environmental impact, all compounds had BCF scores below the threshold value. In the Tox21 pathway, some compounds exhibited moderate to high toxicity for specific targets, while others had no toxic effects. Obtained results of this investigation will be hoped to provide valuable insights into the relationship between ADME, toxicity, and electronic structure in the exploration, development, and improvement of future drug agents.

Acknowledgments

All calculations have been carried out at TUBITAK ULAKBIM, High Performance and Grid Computing Center (TR-Grid e-Infrastructure). The author thanks to Scientific Research Projects Department of Cumhuriyet University (Project No: EĞT-2023-098)

Author Contribution

Goncagül Serdaroğlu, performed all quantum chemical and ADMT computations, data analyses, supervising, writing, and editing.

Ethic

There are no ethical issues with the publication of this article.

Conflict of Interest

The authors declare that they have no known competing financial interests or personal relationships that could have appeared to influence the work reported in this paper.

ORCID

Goncagül Serdaroğlu https://orcid.org/0000-0001-7649-9168

References

Adorjan, B., & Buchbauer, G. (2010). Biological properties of essential oils: An updated review. *Flavour and Fragrance Journal*. *25*(6), 407-426. 4https://doi.org/10.1002/ffj.2024

Ali, J., Camilleri, P., Brown, M. B., Hutt, A. J., & Kirton, S. B. (2012). In silico prediction of aqueous solubility using simple QSPR models: The importance of phenol and phenol-like moieties. *Journal of Chemical Information and Modeling*, *52*, 2950−2957. https://doi.org/10.1021/ci300447c

Bailly, C. (2020). Targets and pathways involved in the antitumor activity of citral and its stereo-isomers. *European Journal of Pharmacology*, *871*, 172945. https://doi.org/10.1016/j.ejphar.2020.172945

Balusamy, S. R., Perumalsamy, H., Veerappan, K., Huq, M. A., Rajeshkumar, S., Lakshmi, T., & Kim, Y. J. (2020). Citral induced apoptosis through modulation of key genes involved in fatty acid biosynthesis in human prostate cancer cells: In silico and in vitro study. *BioMed Research International*, *2020*, 6040727. https://doi.org/10.1155/2020/6040727

Becke, A. D. (1993). A new mixing of Hartree–Fock and local density-functional theories. *Journal of Chemical Physics*, *98*, 1372-1377. https://doi.org/10.1063/1.464304

Bouyahya, A., Guaouguaou, F. E., El Omari, N., El Menyiy, N., Balahbib, A., El-Shazly, M., & Bakri, Y. (2022). Anti-inflammatory and analgesic properties of Moroccan medicinal plants: Phytochemistry, in vitro and in vivo investigations, mechanism insights, clinical evidences and perspectives. *Journal of Pharmaceutical Analysis*, *12*(1), 35-57. https://doi.org/10.1016/j.jpha.2021.07.004

Burdock, G. A., & Carabin, I. G. (2009). Safety assessment of coriander (Coriandrum sativum L.) essential oil as a food ingredient. *Food and Chemical Toxicology*, *47*(6), 1202-1209. https://doi.org/10.1016/j.fct.2008.11.006

Carpenter, J. F., Pikal, M. J., Chang, B. S., & Randolph, T. W. (1997). Rational design of stable lyophilized protein formulations: Theory and practice. *In Pharmaceutical Biotechnology*, *9*, 189-227. https://doi.org/10.1023/A:1012180707283

Cheng, T., Zhao, Y., Li, X., Lin, F., Xu, Y., Zhang, X., Li, Y., & Wang, R. (2007). Computation of octanol−water partition coefficients by guiding an additive model with knowledge. *Journal of Chemical Information and Modeling*, *47*(6), 2140–2148. https://doi.org/10.1021/ci700257y

Daina, A., Michielin, O., & Zoete, V. (2014). iLOGP: A simple, robust, and efficient description of n-octanol/water partition coefficient for drug design using the GB/SA approach. *Journal of Chemical Information and Modeling*, *54*(12), 3284–3301. https://doi.org/10.1021/ci500467k

Daina, A., Michielin, O., & Zoete, V. (2017). SwissADME: A free web tool to evaluate pharmacokinetics, druglikeness and medicinal chemistry friendliness of small molecules. *Scientific Reports, 7*, 42717. https://doi.org/10.1038/srep42717

Delaney, J. S. (2004). ESOL: Estimating aqueous solubility directly from molecular structure. *Journal of Chemical Information and Computer Sciences*, *44*, 1000-1005. https://doi.org/10.1021/ci034243x

Dennington, R., Keith, T. A., & Millam, J. M. (2016). *GaussView, version 6.0.16*. Semichem Inc Shawnee Mission KS.

Egan, W. J., Merz, K. M., Jr., & Baldwin, J. J. (2000). Prediction of drug absorption using multivariate statistics. *Journal of Medicinal Chemistry*, *43*, 3867-3877. https://doi.org/10.1021/jm000292e

Erdogan, M., & Serdaroglu, G. (2021). New Hybrid (E)-4-((pyren-1-ylmethylene)amino)-N-(thiazol-2-yl)benzenesulfonamide as a potential drug candidate: Spectroscopy, TD-DFT, NBO, FMO, and MEP studies. *Chemistry Select*, *6*, 9369–9381. https://doi.org/10.1002/slct.202102602

Frisch, M. J., Trucks, G. W., Schlegel, H. B., Scuseria, G. E., Robb, M. A., Cheeseman, J. R., Scalmani, G., Barone, V., Mennucci, B., Petersson, G. A., Nakatsuji, H., Caricato, M., Li, X., Hratchian, H. P., Izmaylov, A. F., Bloino, J., Zheng, G., Sonnenberg, J. L., Hada, M., Ehara, … Fox, D. J. (2013). *Gaussian 09W, Revision D.01*. Gaussian Inc.

Gaonkar, R., Yallappa, S., Dhananjayac, B. L., & Hegde, G. (2016). Development and validation of reverse phase high-performance liquid chromatography for citral analysis from essential oils. *Journal of Chromatography B*, 1036–1037, 50–56. https://doi.org/10.1016/j.jchromb.2016.10.001

Gazquez, J. L., Cedillo, A., & Vela, A. (2007). Electrodonatingand Electroaccepting Powers. *Journal of Physical Chemistry A*, *111*(10), 1966-1970. https://doi.org/10.1021/jp065459f

Ghose, A. K., Viswanadhan, V. N., & Wendoloski, J. J. (1999). A knowledge-based approach in designing combinatorial or medicinal chemistry libraries for drug discovery. 1. A qualitative and quantitative characterization of known drug databases. *Journal of Combinatorial Chemistry*, *1*, 55-68. https://doi.org/10.1021/cc9800071

Gomez, B., Likhanova, N. V., Domínguez-Aguilar, M. A., Martínez-Palou, R., Vela, A., & Gazquez, J. L. (2006). Quantum chemical study of the inhibitive properties of 2-Pyridyl-Azoles. *Journal of Physical Chemistry B*, *110*(18), 8928-8934. https://doi.org/10.1021/jp057143y

Herzberg, G. (1964). *Molecular spectra and molecular structure III* (1st ed.). D. Van Nostrand Company Inc.

Hill, T. L. (1962). *An introduction to statistical thermodynamics*. Addison-Wesley Publishing.

Hsissou, R., Benhiba, F., Echihi, S., Benzidia, B., Cherrouf, S., Haldhar, R., Alvi, P. A., Kaya, S., Serdaroglu, G., & Zarrouk, A. (2021). Performance of curing epoxy resin as potential anticorrosive coating for carbon steel in 3.5% NaCl medium: Combining experimental and computational approaches. *Chemical Physics Letters*, 783, 139081. https://doi.org/10.1016/j.cplett.2021.139081

Jackson, E., Shoemaker, R., Larian, N., & Cassis, L. (2017). Adipose tissue as a site of toxin accumulation. *Comprehensive Physiology*, *7*(4), 1085–1135. https://doi.org/10.1002/cphy.c160038

Janak, J. F. (1978). Proof that ∂E/∂ni=εin density-functional theory. *Physical Review B*, *18*(12), 7165-7168. https://doi.org/10.1103/PhysRevB.18.7165

Ju, J., Xie, Y., Yu, H., Guo, Y., Cheng, Y., Qian, H., & Yao, W. (2020). Analysis of the synergistic antifungal mechanism of eugenol and citral. *LWT*, *123*, 109128. https://doi.org/10.1016/j.lwt.2020.109128

Koopmans, T. (1934). Über die zuordnung von wellenfunktionen und eigenwertenzu den einzelnen elektronen eines atoms. *Physica*, *1*, 104-113. https://doi.org/10.1016/S0031-8914(34)90011-2

Kudin, K. N., Scuseria, G. E., & Cancès, E. (2002). A black-box self-consistent field convergence algorithm: One step closer. *Journal of Chemical Physics*, *116*(19), 8255-8261. https://doi.org/10.1063/1.1470195

Lee, C., Yang, W., & Parr, R. G. (1988). Development of the Colle-Salvetti correlation-energy formula into a functional of the electron density. *Physical Review B*, *37*, 785-789. https://doi.org/10.1103/PhysRevB.37.785

Li, R. Y., Wu, X. M., Yin, X. H., Long, Y. H., & Li, M. (2015). Naturally produced citral can significantly inhibit normal physiology and induce cytotoxicity on Magnaporthe grisea. *Pesticide Biochemistry and Physiology*, *118*, 19-25. https://doi.org/10.1016/j.pestbp.2014.10.015

Li, X., & Frisch, M. J. (2006). Energy-represented DIIS within a hybrid geometry optimization method. *Journal of Chemical Theory and Computatio*n, *2*(3), 835-839. https://doi.org/10.1021/ct050275a

Lin, J. H., & Lu, A. Y. (1997). Role of Pharmacokinetics and Metabolism in Drug Discovery and Development. *Pharmacological Reviews*, *49*(4), 403-449. https://www.ncbi.nlm.nih.gov/pubmed/9443165

Lipinski, C. A., Lombardo, F., Dominy, B. W., & Feeney, P. J. (2001). Experimental and computational approaches to estimate solubility and permeability in drug discovery and development settings. *Advanced Drug Delivery Reviews*, *46*, 3–26. https://doi.org/10.1016/S0169-409X(00)00129-0

Martin, Y. C. (2005). A bioavailability score. *Journal of Medicinal Chemistry*, *48*, 3164-3170. https://doi.org/10.1021/jm0492002

McGeer, J. C., Brix, K. V., Skeaff, J. M., DeForest, D. K., Brigham, S. I., Adams, W. J., & Green, A. (2003). Inverse relationship between bioconcentration factor and exposure concentration for metals: implications for hazard assessment of metals in the aquatic environment. *Environmental Toxicology and Chemistry*, *22*(5), 1017-1037. https://doi.org/10.1002/etc.5620220509

McLean, A. D., & Chandler, G. S. (1980). Contracted Gaussian-basis sets for molecular calculations. 1. 2nd row atoms, Z=11-18. *Journal of Chemical Physics*, *72*(9), 5639-5648. https://doi.org/10.1063/1.438980

McQuarrie, D. A. (1973). *Statistical thermodynamics.* Harper & Row Publishers.

Muegge, I., Heald, S. L., & Brittelli, D. (2001). Simple selection criteria for drug-like chemical matter. *Journal of Medicinal Chemistry*, *44*(12), 1841–1846. https://doi.org/10.1021/jm015507e

Nendza, M., & Müller, M. (2010). Screening for low aquatic bioaccumulation. 1. Lipinski's 'Rule of 5' and molecular size. *SAR and QSAR in Environmental Research*, *21*(5-6), 495-512. https://doi.org/10.1080/1062936X.2010.502295

Oladeji, O. S., Oluyori, A. P., Bankole, D. T., & Afolabi, T. Y. (2020). Natural products as sources of antimalarial drugs: Ethnobotanical and ethnopharmacological studies. *BioMed Research International*, 2020, 7076139. https://doi.org/10.1155/2020/7076139

Ortiz, M. I., González-García, M. P., Ponce-Monter, H. A., Castañeda-Hernández, G., & Aguilar-Robles, P. (2010). Synergistic effect of the interaction between naproxen and citral on inflammation in rats. *Phytomedicine*, *18*(1), 74-79. https://doi.org/10.1016/j.phymed.2010.05.009

Oyedeji, A. O., Okunowo, W. O., Osuntoki, A. A., Olabode, T. B., & Ayo-folorunso, F. (2020). Insecticidal and biochemical activity of essential oil from Citrus sinensis peel and constituents on Callosobrunchus maculatus and Sitophilus zeamais. *Pesticide Biochemistry and Physiology*, *168*, 104643. https://doi.org/10.1016/j.pestbp.2020.104643

Parr, R. G., & Pearson, R. G. (1983). Absolute hardness: companion parameter to absolute electronegativity. *Journal of the American Chemical Society*, *105*, 7512-7516. https://doi.org/10.1021/ja00364a005

Parr, R. G., Szentpaly, L. V., & Liu, S. (1999). Electrophilicity index. *Journal of the American Chemical Society*, *121*, 1922-1924. https://doi.org/10.1021/ja983494x

Pearson, R. G. (1986). Absolute electronegativity and hardness correlated with molecular orbital theory. *Proceedings of the National Academy of Sciences of the United States of America*, *83*, 8440-8441. https://doi.org/10.1073/pnas.83.22.8440

Perdew, J. P., & Levy, M. (1983). Physical content of the exact Kohn-Sham orbital energies: Band gaps and derivative discontinuities. *Physical Review Letters*, *51*(20), 1884-1887. https://doi.org/10.1103/PhysRevLett.51.1884

Perdew, J. P., Parr, R. G., Levy, M., & Balduz, J. L. (1982). Density-functional theory for fractional particle number: Derivative discontinuities of the energy. *Physical Review Letters*, *49*(23), 1691-1694. https://doi.org/10.1103/PhysRevLett.49.1691

Plata-Rueda, A., Martínez, L. C., da Silva Rolim, G., Pereira Coelho, R., Henrique Santos, M., de Souza Tavares, W., Cola Zanuncio, J., & Serrão, J. E. (2020). Insecticidal and repellent activities of Cymbopogon citratus (Poaceae) essential oil and its terpenoids (citral and geranyl acetate) against Ulomoides dermestoides. *Crop Protection*, *137*, 105299. https://doi.org/10.1016/j.cropro.2020.105299

Raghavachari, K., Binkley, J. S., Seeger, R., & Pople, J. A. (1980). Self-Consistent Molecular Orbital Methods. 20. Basis set for correlated wave-functions. *Journal of Chemical Physics*, 72(1), 650-654. https://doi.org/10.1063/1.438955

Ruiz Perez-Cacho, P., & Rouseff, R. (2008). Processing and storage effects on orange juice aroma: A review. *Journal of Agricultural and Food Chemistry*, *56*(21), 9785-9796. https://doi.org/10.1021/jf801244j

Samarghandian, S., Shoshtari, M. E., Sargolzaei, J., Hossinimoghadam, H., & Azad Farahzad, J. (2014). Anti-tumor activity of safranal against neuroblastoma cells. *Pharmacognosy Magazine*, *10*(Suppl 2), S419-S424. https://doi.org/10.4103/0973-1296.133296

Serdaroğlu, G. (2011). A DFT study of determination of the reactive sites of the acetylcholine and its agonists: In the gas phase and dielectric medium. *International Journal of Quantum Chemistry*, *111*(10) 2464-2475. https://doi.org/10.1002/qua.22512

Serdaroğlu, G. (2011). DFT and Ab initio computational study on the reactivity sites of the GABA and its agonists, such as CACA, TACA, DABA, and muscimol: In the gas phase and dielectric media. *International Journal of Quantum Chemistry*, *111*(14), 3938-3948. https://doi.org/10.1002/qua.22809

Serdaroglu, G., & Durmaz, S. (2010). DFT and statistical mechanics entropy calculations of diatomic and polyatomic molecules. *Indian Journal of Chemistry*, 49, 861-866. http://nopr.niscpr.res.in/handle/123456789/9918

Serdaroğlu, G., & Ortiz, J. V. (2017). Ab initio calculations on some antiepileptic drugs such as phenytoin, phenbarbital, ethosuximide and carbamazepine. *Structural Chemistry*, *28*(4), 957-964. https://doi.org/10.1007/s11224-016-0898-3

Serin, S. (2022). DFT-based computations on some structurally related N-substituted piperazine. *Journal of the Indian Chemical Society*, *99*, 100766. https://doi.org/10.1016/j.jics.2022.100766

Serin, S. (2023). A comprehensive DFT study on organosilicon-derived fungicide flusilazole and its germanium analogue: A computational approach to Si/Ge bioisosterism. *Journal of the Indian Chemical Society*, *100*, 100939. https://doi.org/10.1016/j.jics.2023.100939

Serin, S., Kaya, G., & Utku, T. (2022). Insights into solvent effects on molecular properties, physicochemical parameters, and NLO behavior of brinzolamide, a bioactive sulfonamide: A computational study. *Journal of the Indian Chemical Society*, *99*, 100738. https://doi.org/10.1016/j.jics.2022.100738

Sharma, A. D., & Kaur, I. (2023). Targeting penicillin binding proteins (PBPs) by using bioactive geranial from essential oil of Cymbopogan pendulus against gram-positive and gram-negative bacteria: Molecular docking and experimental approach. *Bulgarian Chemical Communications*, *55*(1), 40-47. http://www.bcc.bas.bg/BCC_Volumes/Volume_55_Number_1_2023/bcc-55-1-2023.pdf#page=38

Sharmeen, J. B., Mahomoodally, F. M., Zengin, G., & Maggi, F. (2021). Essential oils as natural sources of fragrance compounds for cosmetics and cosmeceuticals. *Molecules*, *26*, 666. https://doi.org/10.3390/molecules26030666

Silva, B. I. M., Nascimento, E. A., Silva, C. J., et al. (2021). Anticancer activity of monoterpenes: A systematic review. *Molecular Biology Reports*, *48*, 5775-5785. https://doi.org/10.1007/s11033-021-06578-5

Tchoumbougnang, F., Amvam Zollo, P. H., Dagne, E., & Mekonnen, Y. (2005). In vivo antimalarial activity of essential oils from Cymbopogon citratus and Ocimum gratissimum on mice infected with Plasmodium berghei. *Planta Medica*, *71*(1), 20-23. https://doi.org/10.1055/s-2005-837745

Veber, D. F., Johnson, S. R., Cheng, H.-Y., Smith, B. R., Ward, K. W., & Kopple, K. D. (2002). Molecular properties that influence the oral bioavailability of drug candidates. *Journal of Medicinal Chemistry*, *45*, 2615-2623. https://doi.org/10.1021/jm020017n

Viktorová, J., Stupák, M., Reho˘rov ˘ á, K., Dobiasová, S., Hoang, L., Hajšlová, J., Van Thanh, T., Van Tri, L., Van Tuan, N., & Rum, T. (2020). Lemon grass essential oil does not modulate cancer cells multidrug resistance by citral—its dominant and strongly antimicrobial compound. *Foods*, *9*, 585. https://doi.org/10.3390/foods9050585

Wildman, S. A., & Crippen, G. M. (1999). Prediction of physicochemical parameters by atomic contributions. *Journal of Chemical Information and Computer Sciences*, *39*, 868-873. https://doi.org/10.1021/ci990307l

Wohlmuth, H., Smith, M. K., Brooks, L. O., Myers, S. P., & Leach, D. N. (2006). Essential oil composition of diploid and tetraploid clones of ginger (Zingiber officinale Roscoe) grown in Australia. *Journal of Agricultural and Food Chemistry*, *54*(4), 1414–1419. https://doi.org/10.1021/jf0521799

Zeng, R., Zou, X., Huang, C., Si, H., Song, J., Zhang, J., Luo, H., Wang, Z., Wang, P., Fan, G., Rao, X., Liao, S., & Chen, S. (2023). Novel design of citral-thiourea derivatives for enhancing antifungal potential against Colletotrichum gloeosporioides. *Journal of Agricultural and Food Chemistry*, *71*(7), 3173-3183. https://doi.org/10.1021/acs.jafc.2c07851